Research article

Sustainable development of fuel cell using enhanced weighted mean of vectors algorithm

Manish Kumar Singla [a], Jyoti Gupta [b], Parag Nijhawan [b], Mohammed H. Alsharif [c], Mun-Kyeom Kim [d],[*]

[a] Department of Interdisciplinary Courses in Engineering, Chitkara University Institute of Engineering & Technology, Chitkara University, Punjab, India
[b] Electrical and Instrumentation Engineering Department, Thapar Institute of Engineering and Technology, Patiala, India
[c] Department of Electrical Engineering, College of Electronics and Information Engineering, Sejong University, 209 Neungdong-ro, Gwangjin-gu, Seoul 05006, South Korea
[d] School of Energy System Engineering, Chung-Ang University, 84 Heukseok-ro, Dongjak-gu, Seoul 06974, South Korea

ARTICLE INFO

ABSTRACT

Using the mathematical model of a Direct Methanol Fuel Cell (DMFC) stack, a new optimum approach is presented for estimating the seven unknown parameters i.e., (e_o, α, R, j_{eid}, C_1, β, r_{eq}) optimally. Specifically, a method is proposed for minimization of the Sum of Squared Errors (SSE) associated with the estimated polarization profile, based on the experimental data from simulations. The Enhanced Weighted mean of vectors (EINFO) algorithm is a novel metaheuristic method that is proposed to achieve this goal. An analysis of the results of this method is then compared to various metaheuristic algorithms such as the Particle Swarm Optimization (PSO), Sine Cosine Algorithm (SCA), Dragonfly Algorithm (DA), Atom Search Optimization (ASO), and Weighted mean of vectors (INFO) well known in literature. As a final step to confirm the proposed approach's effectiveness, the sensitivity analysis is carried out using temperature changes, along with comparison against different approaches described in the literature to demonstrate its superiority. After comparison of parameter estimation and different operating temperature a non-parametric test is also performed and compared with the rest of the metaheuristic algorithms used in the manuscript. From these tests it is concluded that the proposed algorithm is superior to the rest of the compared algorithms.

1. Introduction

A growing number of research projects are devoted to environmental and ecological issues [1–3]. Research in this area is focused on developing clean energy sources, which is most important. The low carbon footprint and efficiency of fuel cells make them one of the most preferred energy sources today. Additionally, the production of electricity from fuel cells is not influenced by the weather, unlike that of solar and wind energy sources. Direct methanol fuel cell technology will be the main emphasis (DMFC). This fuel cell is regarded as one of the top rivals for low power applications (from less than a watt to several megawatts) because to its liquid fuel and minimal CO_2 emissions, as well as low activation temperature.

---

* Corresponding author.
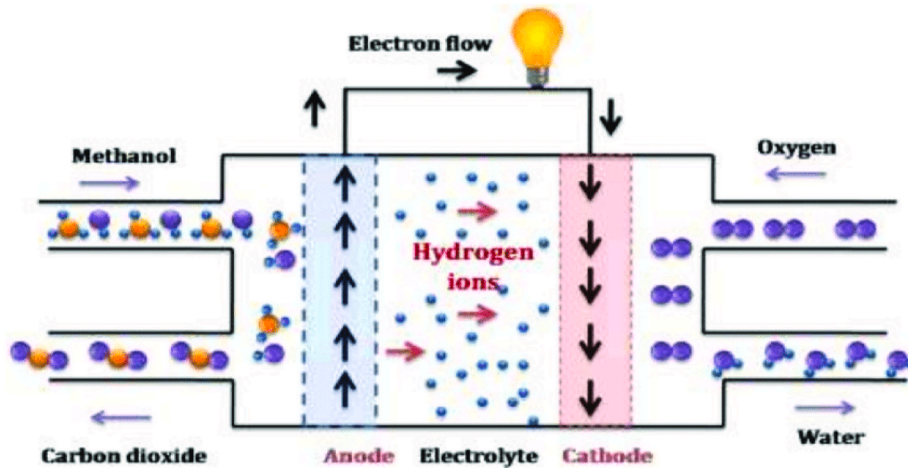 *E-mail address:* mkim@cau.ac.kr (M.-K. Kim).

Fig. 1. Schematic of DMFC [28].

In order to examine the performance-affecting factors for DMFC cells, analytical models [4–8], semi-empirical equations [9–13], and mechanistic models [14–21] have all been taken into account. One of the main areas of interest is semi-empirical models. Yang et al. [11] developed a fuel cell model with an equivalent circuit that successfully addresses nonlinear resistors, capacitors, and an inductor. A model of a DMFC type fuel cell was published by Yang et al. [12] that takes into account four operating parameters, such as temperature, methanol concentration, and methanol and air flow rates.

Compared to the PEMFC and SOFC fuel cells, the number of publications in the literature devoted to the modelling of the DMFC seems to be quite minimal. Mostly researchers estimate the unknown parameters using meta heuristic algorithm like swam based algorithms [22,23], genetic based algorithms [24] and currently focusing on artificial intelligence based algorithms [25,26]. Most of these works have had great difficulty in solving the Butler–Volmer equation. To make the intricacy of this equation simpler in their writings, the authors use assumptions and approximations. The performance of the models suggested for retracing experimental data of the current density curve and stack voltage (J-V) of DMFC stacks may be adversely affected by the application of certain approximations and assumptions. The key optimization approach used in earlier publications for parameter extraction is Newton-Raphson [9–13]. The drawback of this type of optimization strategy is that it has demonstrated a high sensitivity to beginning values and is difficult to differentiability and convexity. Researchers also noted that metaheuristic methods were not used for the extraction of parameters from the DMFC stack models, despite the fact that these approaches were demonstrated to conduct optimization better than other optimization strategies. They may, for instance, be used to extract properties from models of solar cells, PEMFC [27], SOFC fuel cells, and other systems. The paper's main contribution is outlined in the highlights below:

- Using a distinct EINFO methodology, the DMFC model's parameters are optimally retrieved.
- Real experimental data collected in various climatic conditions are used to confirm the performance of the proposed strategy, which is then compared to other well-established approaches.
- The calculation time of the fuel cell model is computed in order to evaluate the effectiveness and precision of the suggested algorithm.
- To check the consistency and robustness of the proposed algorithm the convergence curve, and different operating temperature, results are obtained.
- Non-parametric statistical test i.e., Friedman Ranking Test, Wilcoxon rank sum test is done for finding the significance of parameter estimation of DMFC.

2. DMFC mathematical modeling

In a fuel cell, chemical energy is transformed into electrical energy. It continuously converts chemical energy into electrical energy and heat. The fuel cell transforms the chemical energy provided by a fuel and an oxidant into water and electrical energy. The fuel cell is different from a battery in that it runs constantly while receiving fuel rather than storing energy. The mathematical modelling of the DMFC stack is our goal and schematic of DMFC is represented in Fig. 1. To extract the model's unidentified parameters i.e., (e_o, α, R, j_{eid}, C_1, β, r_{eq}), the EINFO metaheuristic algorithm is adopted. The DMFC cell voltage is represented in equation (1) [10].

$$v_{cell} = E_{act} - E_{con} - E_{rev} - E_{ohm} \tag{1}$$

Where the cell voltage is represented by v_{cell}, the concentration polarization is represented by E_{con}, the activation polarization is represented by E_{act}, the reversible polarization is represented by E_{rev}, and the ohmic polarization is represented by E_{ohm}.

The electrochemical equation of DMFC is given in following equations:

Equation (2) represents the anode side electrochemical reaction:

$$CH_3OH + H_2O \rightarrow 6H^+ + 6e^- + CO_2 \tag{2}$$

Equation (3) represents the cathode side electrochemical reaction:

$$\frac{3}{2}O_2 + 6H^+ + 6e^- \rightarrow 3H_2O \tag{3}$$

Equation (4) represents the overall electrochemical reaction:

$$CH_3OH + \frac{3}{2}O_2 \rightarrow 2H_2O + CO_2 + Heat \tag{4}$$

(a) Expression for Activation Loss Voltage:

The overvoltage needed to energize the electrodes is represented by the activation voltage. Using the Butler-Volmer equation, the current density j_{max} will be expressed in equation (5) to estimate the value of the activation voltage [9]:

$$j_{max} = j_{eid}\left[e^{\left(\frac{\alpha nF}{RT}E_{act}\right)} - e^{-\left(\frac{(1-\alpha)F}{RT}E_{act}\right)}\right] \tag{5}$$

Where exchange current density is represented by j_{eid}, and the value of α lies between the 0 and 1. The calculation of the activation voltage of equation (5) cannot be solved analytically in its current form. The voltage E_{act} will be replaced by E_{con}, E_{rev}, E_{ohm}, and v_{cell} in the first exponential of the equation to solve this problem, which results in the following equation (6):

$$j_{max} = j_{eid}\left[e^{\left(\frac{\alpha nF}{RT}(E_{con}-E_{ohm}-E_{rev}-v_{cell})\right)} - e^{-\left(\frac{(1-\alpha)nF}{RT}E_{act}\right)}\right] \tag{6}$$

Finally, the expression for the new activation voltage may be expressed in equation (7):

$$E_{act} = \frac{RT\left[\log\left(j_{max} + j_{eid}e^{\left(\frac{\alpha nF}{RT}(E_{con}-E_{ohm}-E_{rev}-v_{cell})\right)}\right) - \log(j_{eid})\right]}{\alpha nF} \tag{7}$$

(b) Expression for Ohmic Loss Voltage:

The term "ohmic loss voltage" refers to the resistances that are added in response to the movement of ions, electrons, and material across a membrane. The following equation (8) represents the ohmic voltage [10]:

$$E_{ohm} = Rj_{cd} \tag{8}$$

Where the internal resistance of the fuel cell is represented by R, and he current density is denoted by j_{cd}.

(c) Expression for Concentration Loss Voltage:

The voltage loss due to mass transportation is indicated by the voltage loss of concentration. The concentration voltage may be expressed in equation (9) using Fick's law [12]:

$$E_{con} = -\frac{RT}{\beta nF}\ln\left(1 - \frac{j_{max}}{j_{limit}}\right) \tag{9}$$

In equation (9) j_{max} is briefly represented in equation (10):

$$j_{max} = \frac{E_{rev} - v_{cell} - Rj_{cd}}{r_{con} + r_{act}} \tag{10}$$

Where the empirical coefficient parameter is denoted by β, and the limit current density is represented by j_{limit}.

(d) Expression for Reversible Loss Voltage:

The energetic activity in the fuel cell, which includes the forming and breaking of bonds at the level of the electrodes, leads to the reversible voltage. The Nernst equation may be used to explain the reversible voltage as shown in equation (11) [21]:

$$E_{rev} = e_o + \frac{RT}{nF}\left[\log(c_{CH_3OH}) + \frac{3}{2}\log(p_{o_2})\right] - \frac{RT}{nF}\left[2\log(p_{H_2O}) + \frac{3}{2}\log(p_{co_2})\right] \tag{11}$$

Where e_o is the potential for the reaction between methanol and oxygen, p_{CH_3OH} is the partial pressure of methanol present at the anode, p_{H_2O} is the partial pressure of water at the cathode, which is 1, when liquid water is produced, p_{o_2} is the partial pressure of oxygen at the cathode, is p_{co_2} the partial pressure CO_2, R is the universal gas constant (8.314 J/molK), F is the Faraday's constant (94,485 c/mol) and number of electrons is represented by n. In general, experimental access to the pressures of CO_2 and H_2O is not possible. Due to these factors, the term $-\frac{RT}{nF}\left[2\log(p_{H_2O}) + \frac{3}{2}\log(p_{c_2o})\right]$ will equal C_1, making C_1 a parameter that has to be established. The reversible voltage equation therefore becomes as shown in equation (12):

$$E_{rev} = e_o + \frac{RT}{nF}\left[\log(c_{CH_3OH}) + \frac{3}{2}\log(p_{o_2})\right] + C_1 \tag{12}$$

Where the temperature of cell in K (Kelvin) is denoted by T.

(e) Expression for Fuel Cell Voltage:

Based on previous theoretical developments, the following equation (13) can be the expression of the fuel cell voltage V_{cell}:

$$v_{cell} = E_{act} - E_{con} - E_{rev} - E_{ohm} \tag{13a}$$

With

$$E_{act} = \frac{RT\left[\log\left(j_{max} + j_{eid}e^{\left(\frac{\alpha nf}{rt}(E_{con} - E_{ohm} - E_{rev} - v_{cell})\right)}\right) - \log(j_{eid})\right]}{\alpha nF} \tag{13b}$$

$$E_{ohm} = Rj_{cd} \tag{13c}$$

$$E_{con} = -\frac{RT}{\beta nF}\ln\left(1 - \frac{j_{max}}{j_{limit}}\right) \tag{13d}$$

$$E_{rev} = e_o + \frac{RT}{nF}\left[\log(c_{CH_3OH}) + \frac{3}{2}\log(p_{o_2})\right] + C_1 \tag{13e}$$

The seven unknown parameters y are given by equations (13a-13e) in the form y = $[e_o, \alpha, R, j_{eid}, C_1, \beta, r_{eq}]$.

2.1. Problem formulation

For the purpose of estimating the parameters of DMFC, this research suggests a new, better approach called EINFO. Utilizing optimization methods, output voltage is predicted for each input of current density. Equation (14) illustrates the objective function of the SSE (Sum of Square Error) metric, which is used to compare predicted and experimental output voltages.

$$SSE = MIN\left(F = \sum_{i=1}^{N}(V_{actual} - V_i)^2\right) \tag{14}$$

The constraints of the DMFC is represented in equations 15–21:

$$e_{omin} \leq e_o \leq e_{omax} \tag{15}$$

$$\beta_{min} \leq \beta \leq \beta_{max} \tag{16}$$

$$\alpha_{min} \leq \alpha \leq \alpha_{max} \tag{17}$$

$$R_{min} \leq R \leq R_{max} \tag{18}$$

$$j_{eid\,min} \leq j_{eid} \leq j_{eid\,max} \tag{19}$$

$$r_{eqmin} \leq r_{eq} \leq r_{eqmax} \tag{20}$$

$$C_{1\,min} \leq C_1 \leq C_{1\,max} \tag{21}$$

Where N represents the number of data points V_{actual} is the experimental output voltage and V_i is the predicted output voltage using various optimization algorithms. The main goal of this paper is to minimize the SSE value for obtaining better performance as well as more accuracy and precision in order to estimate the parameters of DMFC.

3. Method

In this part, the suggested improved INFO (EINFO) algorithm is provided after a brief description of the weighted mean of vectors (INFO) methodology.

3.1. Weighted mean of vectors (INFO)

In 2022, the INFO method was presented [29]. Using four key stages—initialization, updating rule, vector combining, and lastly local search—this technique's concept relies on a strong structure and updating the vectors' positions.

Step 1.   Initialization Stage: A population of n vectors in a D-dimensional search space compensate the INFO approach. The following equation (22) produces a random beginning population:

$$X_n = X_{min} + rand(0, 1).(X_{max} - X_{min}) \tag{22}$$

Where X_n is the nth vector, X_{min}, X_{max} are the limits of the solution domain in each problem and $rand(0, 1)$ is a random number defined in the range of [0, 1].

Step 2.   Updating Rule: Through the search process, this step broadens the population. This operation produces new vectors by using the weighted mean of the vectors. The following equation (23) is the updating rule's key formulation:

if $rand < 0.5$ $\tag{23}$

$$z1_l^{iter} = x_l^{iter} + \sigma \times MeanRule + randn \times \frac{\left(x_{bs} - x_{a1}^{iter}\right)}{(f(x_{bs}) - f(x_{a1}^{iter}) + 1)}$$

$$z2_l^{iter} = x_{bs} + \sigma \times MeanRule + randn \times \frac{\left(x_{a1}^{iter} - x_b^{iter}\right)}{(f(x_{a1}^{iter}) - f(x_{a2}^{iter}) + 1)}$$

else

$$z1_l^{iter} = x_a^{iter} + \sigma \times MeanRule + randn \times \frac{\left(x_{a2}^{iter} - x_{a3}^{iter}\right)}{(f(x_{a2}^{iter}) - f(x_{a3}^{iter}) + 1)}$$

$$z2_i^{iter} = x_{bt} + \sigma \times MeanRule + randn \times \frac{\left(x_{a1}^{iter} - x_{a2}^{iter}\right)}{(f(x_{a1}^{iter}) - f(x_{a2}^{iter}) + 1)}$$

end

Where $z1_l^{iter}$ and $z2_l^{iter}$ denote the new vectors in the gth generation; and σ is the scaling rate of a vector, as shown in equation (24) as:

$$\sigma = 2\alpha \times rand - \alpha \tag{24}$$

Step 3.   Vector Combining: The two vectors generated in the preceding section ($z1_l^{iter}$ and $z2_l^{iter}$) (and) are merged with vector x_l^{iter} based on the INFO method to build the population's diversity as shown in equation 25.1–25.3:

if $rand < 0.5$

if $rand < 0.5$

$$u_l^{iter} = z1_l^{iter} + \mu.\left|z1_l^{iter} - z2_l^{iter}\right| \tag{25.1}$$

else

$$u_l^{iter} = z2_l^{iter} + \mu.\left|z1_l^{iter} - z2_l^{iter}\right| \tag{25.2}$$

end
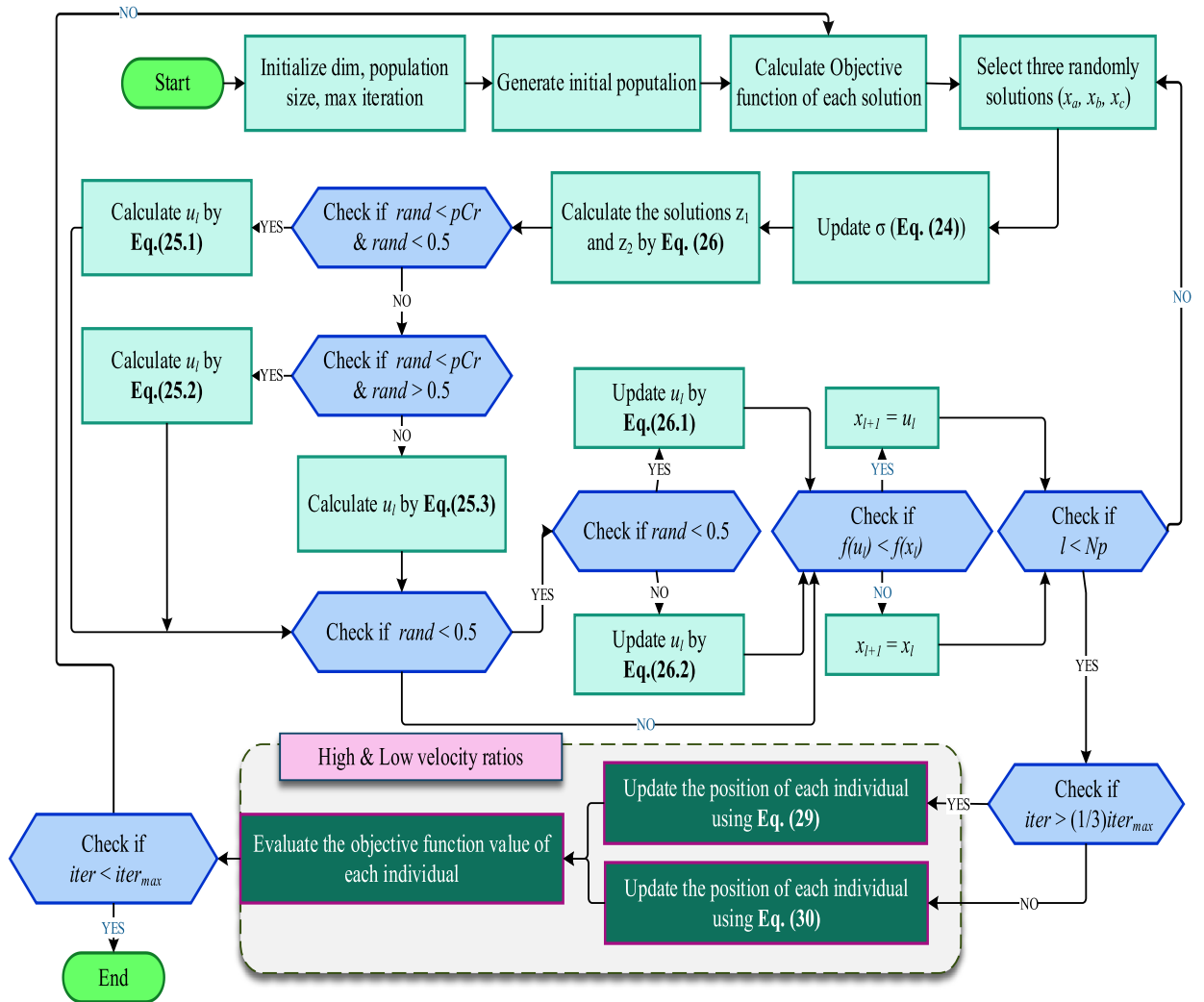
else

$$u_l^{iter} = x_l^{iter} \tag{25.3}$$

end

Figure 2. Proposed algorithm flowchart.

Where μ is equal to $0.05 \times randn$.

Step 4. Local Search: The capability of this stage prevent the algorithm to drop into local minima. The local operator is considered using the global location (x_{best}^{iter}). According to this operator, a novel vector can be produced around global position (x_{best}^{iter}) as shown in equation 26.1 to 26.4:

if $rand < 0.5$

if $rand < 0.5$

$$u_l^{iter} = x_{bs} + randn \times \left(MeanRule + randn \times \left(x_{bs}^{iter} - x_{a1}^{iter} \right) \right)$$ (26.1)

else

$$u_l^{iter} = x_{rnd} + randn \times \left(MeanRule + randn \times \left(v_1 \times x_{bs} - v_2 \times x_{rnd} \right) \right)$$ (26.2)

end

end

$$x_{rnd} = \varphi \times x_{avg} + (1 - \varphi) \times \left(\varphi \times x_{bt} + (1 - \varphi) \times x_{bs} \right)$$ (26.3)

Step 1 Initialization

Set the initial parameters (dim, population, size, maximum iteration)

Generate initial population

Calculate the objective function of each vector

Determine the best vector

Step 2 Updating Rule

Calculate the vector $Z1_i^{iter}$ & $Z2_i^{iter}$ using equation 23

Step 3 Vector Combining

Calculate the vector U_i^{iter} using equation 25

Step 4 Local Search

Calculate the local search operate using equation 26

Step 5 High & low velocity ratio

for iter < 1/3 iter max

Calculate the high velocity ration using equation 27

Update the best vector

then

for iter > 1/3 iter max

Calculate the low velocity ration using equation 29

Update the best vector

Step 6 Return Vector $X_{best,j}^g$ as the final solution

Fig. 3. Pseudocode of EINFO

Table 1
Data sheet of DMFC [10].

Model	Data
Surface of Plate A [cm^2]	25
Cathode Side Oxygen Pressure [bar]	1.35
Reservoir Side Oxygen Pressure [bar]	1.5
Oxygen Flowrate [ml/min]	200
Methanol Flowrate [ml/min]	1.94
Temperature [°C]	80

Table 2
DMFC upper and lower bounds [10].

Parameters	Lower Bound	Upper Bound
e_o (V)	0.83	1.23
α	0	1
R	0	3
j_{eid}	0	0.3
C_1	−4.8	−0.5
β	0	2
r_{eq}	0	50

Table 3
DMFC parameter estimation.

Parameters/Algorithms	PSO	DA	ASO	SCA	INFO	Proposed Algorithm (EINFO)
e_o (V)	0.8458	0.8574	1.2259	1.2299	0.8965	0.8994
α	0.5231	0.4587	0.5507	0.2598	0.3587	0.8879
R	2.9587	1.2410	1.3258	1.5423	1.0028	1.2054
j_{eid}	0.1254	0.1248	0.2194	0.1592	0.1249	0.1670
C_1	−0.8955	−0.1131	−0.8532	−0.1131	−0.9416	−0.5814
β	0.1368	0.5743	0.2587	1.2305	0.1574	1.5840
r_{eq}	12.716	21.078	15.557	12.711	16.171	14.258
SSE	**1.54E-02**	**1.04E-04**	**1.31E-04**	**1.12E-03**	**1.57E-08**	**1.77E-10**
Computation Time (Sec)	**2.908**	**1.589**	**1.897**	**1.995**	**1.115**	**1.252**

$$x_{avg} = \frac{(x_a + x_b + x_c)}{3} \tag{26.4}$$

Where φ is a random number in the range of (0, 1); and x_{rnd} is a new solution that combines the components of the three solutions (x_{avg}, x_{bt} and x_{bs}) randomly. This increases the randomness nature of the proposed algorithm to better search in the solution space. v_1 and v_2 are two random numbers given by the following equation 26.5–26.6:

$$v_1 = \begin{cases} 2 \times rand & if p > 0.5 \\ 1 & otherwise \end{cases} \tag{26.5}$$

$$v_2 = \begin{cases} rand & if p < 0.5 \\ 1 & otherwise \end{cases} \tag{26.6}$$

Where p refers to a random number in the range of (0, 1).

3.2. Proposed enhanced efficient optimization (EINFO) algorithm

The development is called the high and low velocity ratios based on the Marine predator algorithm (MPA) [30,31]. This way was proposed to solve the possibility of the optimal value may drop into local minima. This modification depends on two stages. The first stage is the high-velocity ratio situation. This stage's mathematical model is shown in equation 27.1 to 27.3:

$$iter < \frac{1}{3} iter_{max} \tag{27.1}$$

$$S = \overrightarrow{R_B} \otimes \left(E - \overrightarrow{R_B} \otimes X_n(iter) \right) \tag{27.2}$$

$$X_n(iter+1) = X_n(iter) + P.\overrightarrow{R_B} \otimes S \tag{27.3}$$

Where $\overrightarrow{R_B}$ is a vector of random integers from the Normal distribution that reflect Brownian motion. The notation $\otimes$ depicts entry-by-entry multiplications. The new position is simulated by multiplying $\overrightarrow{R_B}$ by previous position, $P = 0.5$ is a constant, and $\overrightarrow{R_B}$ is a vector of uniform random values in the range [0, 1]. This situation occurs during the first third of iterations when the step size is large, indicating a high level of exploratory ability. *iter* is the current iteration while *iter_{max}* is the maximum one. The fittest solution (E) is designated as a best position to form a matrix as shown in equation (28):

$$E = \begin{bmatrix} Xb_{1.1}^{iter} & \cdots & Xb_{1.d}^{iter} \\ \vdots & \ddots & \vdots \\ Xb_{n.1}^{iter} & \cdots & Xb_{n.d}^{iter} \end{bmatrix} \tag{28}$$

Where, *Xb* denotes the best solution, which is copied n times to create the E matrix. n denotes the number of search agents, whereas d denotes the number of dimensions.

The second stage is the low velocity ratio. This stage occurs near the end of the optimization process, which is typically associated with high exploitation capability. Lévy is the best approach for low-velocity ratios. This stage is depicted as shown in equation 29.1 to 29.3:

$$iter > \frac{1}{3} iter_{max} \tag{29.1}$$

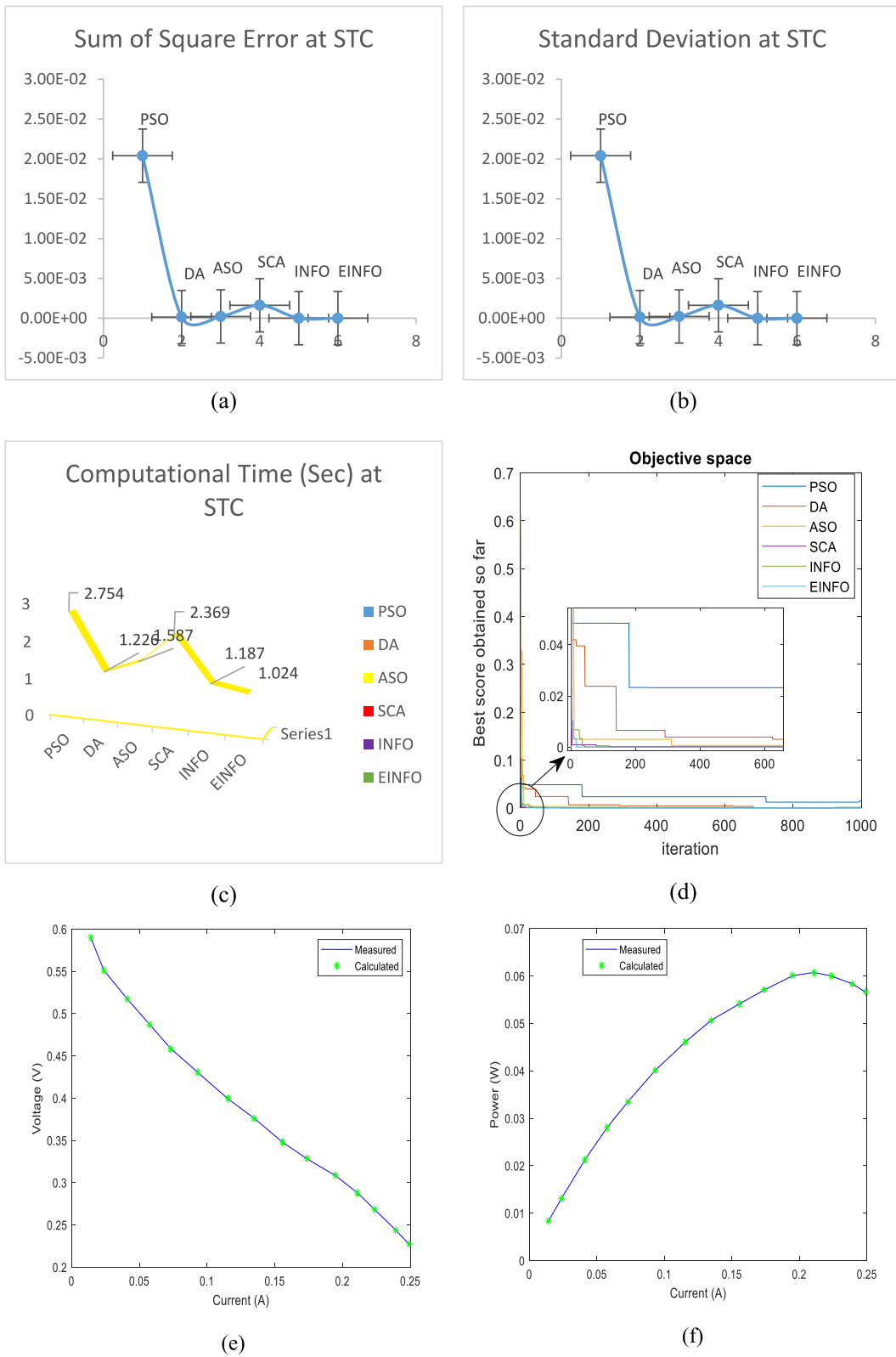$$S = \overrightarrow{R_L} \otimes \left(\overrightarrow{R_L} \otimes E - X_n(iter) \right) \tag{29.2}$$

Fig. 4. (a) Sum of Square Error (b) Standard Deviation (c) Computational Time (d) Convergence Curve at STC (e) V–I Graph (f) P–I Graph.

Table 4
DMFC statistical results.

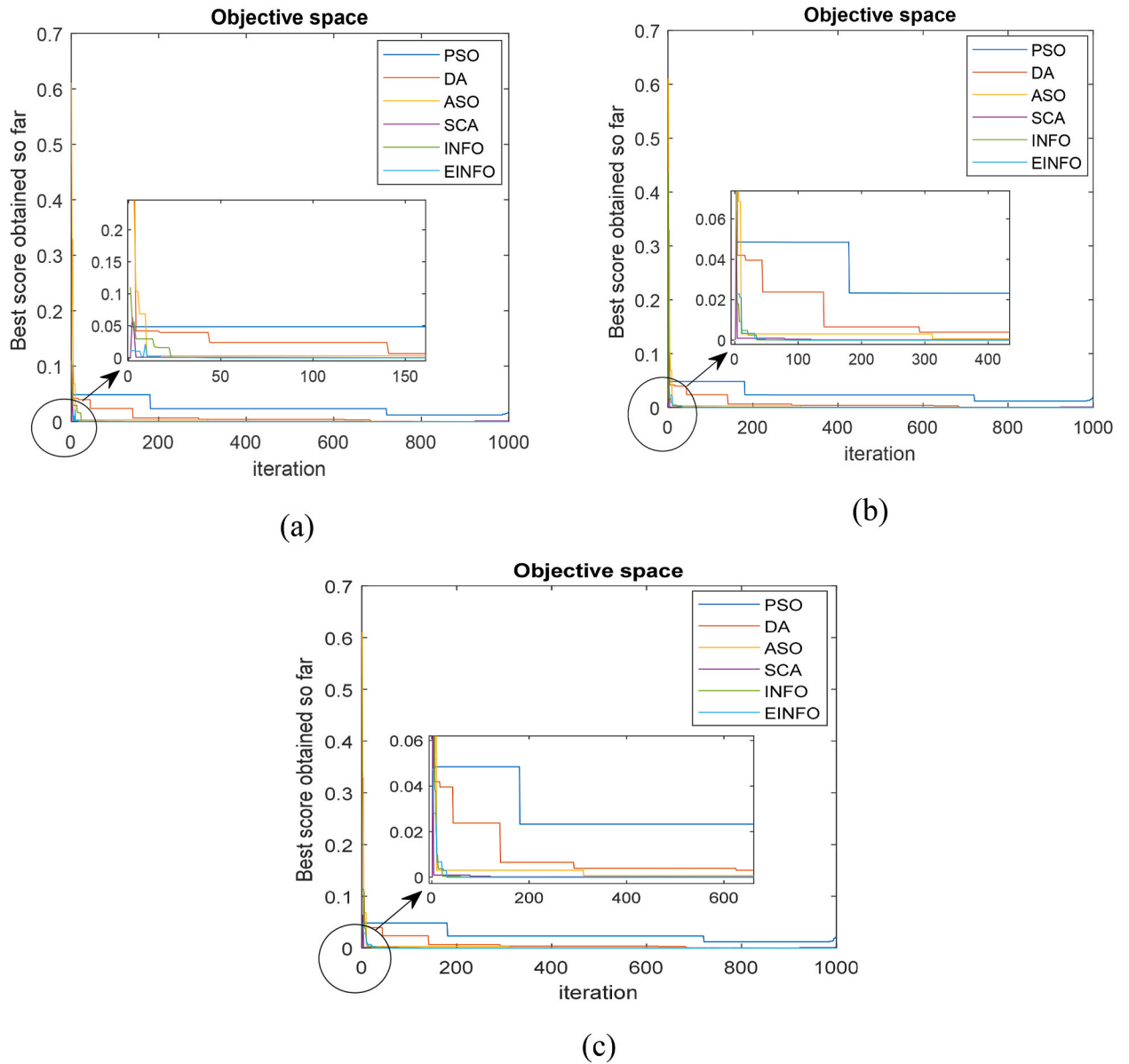| Parameters/Algorithms	PSO	DA	ASO	SCA	INFO	Proposed Algorithm (EINFO)
Minimum	1.54E-02	1.04E-04	1.31E-04	1.12E-03	1.57E-08	1.77E-10
Maximum	2.35E-02	1.47E-04	2.19E-04	2.40E-03	6.49E-08	5.34E-10
Average	1.90E-02	1.27E-04	1.79E-04	1.56E-03	3.34E-08	2.89E-10
Standard Deviation (S.D)	3.16E-03	1.72E-05	3.85E-05	5.16E-04	2.12E-08	1.48E-10

(a)

(b)

(c)

Fig. 5. (a) Convergence Curve at 60 °C (b) 70 °C (c) 90 °C.

Table 5
Parameter estimation of DMFC at different operating temperature.

Temperature (°C)	Parameters/Algorithms	PSO	DA	ASO	SCA	INFO	Proposed Algorithm (EINFO)
60	e_o (V)	0.2589	0.3587	0.4528	0.5478	0.2148	0.2105
	α	0.1048	0.3326	0.3888	0.2673	0.2002	0.3301
	R	1.0251	1.2412	2.2358	2.9587	2.6687	2.0627
	j_{eid}	0.1670	0.1766	0.2255	0.1597	0.1148	0.1282
	C_1	−0.9416	−0.9816	−0.4070	−0.9066	−0.4117	−0.8773
	β	0.1360	0.0400	0.0381	0.0321	0.0241	0.0341
	r_{eq}	16.171	17.754	22.160	15.759	11.538	12.325
	SSE	**1.69E-02**	**1.17E-04**	**1.62E-04**	**1.16E-03**	**1.65E-08**	**1.82E-10**
	Computation Time (Sec)	**2.748**	**1.874**	**1.991**	**2.054**	**1.158**	**1.021**
70	e_o (V)	0.3254	0.8914	0.5897	1.1258	0.5968	0.2358
	α	0.1105	0.5874	0.1997	0.2625	0.3024	0.3425
	R	1.0254	2.8950	2.0336	1.0327	2.0517	1.1691
	j_{eid}	0.1592	0.2354	0.1648	0.1891	0.1161	0.1955
	C_1	−0.8532	−0.2893	−0.1115	−0.9162	−0.7818	−0.9298
	β	0.0574	0.5210	0.1203	0.2802	0.2925	0.3177
	r_{eq}	15.887	23.921	16.936	18.944	11.308	19.253
	SSE	**1.89E-02**	**1.26E-04**	**1.64E-04**	**1.49E-03**	**2.51E-08**	**2.35E-10**
	Computation Time (Sec)	**2.895**	**2.166**	**2.591**	**1.291**	**1.258**	**1.113**
90	e_o (V)	0.5987	0.6587	0.5621	0.3254	0.3210	0.4897
	α	0.1124	0.2707	0.2898	0.3289	0.4543	0.2901
	R	1.0008	1.0587	1.1225	2.5332	1.2705	1.2243
	j_{eid}	0.1249	0.2358	0.1483	0.1757	0.2297	0.1465
	C_1	−0.1131	−0.8532	−0.1154	−0.1066	−0.1173	−0.1163
	β	0.1362	0.2970	0.2561	0.2571	0.4532	0.1407
	r_{eq}	12.711	23.694	14.431	17.454	22.255	14.243
	SSE	**2.04E-02**	**1.39E-04**	**2.17E-04**	**1.62E-03**	**4.50E-08**	**3.18E-10**
	Computation Time (Sec)	**2.754**	**1.226**	**1.587**	**2.369**	**1.187**	**1.024**

$$X_n(iter+1) = E + P.CF \bigotimes S \qquad (29.3)$$

In the Lévy method, multiplying R_L and E, whereas adding the step size to position to aid in the updating of location. The fittest solution (E) is designated as a best position to form a matrix as shown in equation (30):

$$E = \begin{bmatrix} Xb_{1.1}^{iter} & \cdots & Xb_{1.d}^{iter} \\ \vdots & \ddots & \vdots \\ Xb_{n.1}^{iter} & \cdots & Xb_{n.d}^{iter} \end{bmatrix} \qquad (30)$$

Additional feature of EINFO is increasing the chances of escape from local optima. The Fig. 2 and Fig. 3 depicts the flowchart and pseudocode of proposed algorithm, respectively. The place of high and low velocity ratios in the proposed algorithm are presented in this figure. This modification leads to enhance the exploration of the proposed EINFO algorithm.

Step 1.   Initialization

Set the initial parameters (dim, population, size, maximum iteration)
Generate initial population
Calculate the objective function of each vector
Determine the best vector

Step 2.   Updating Rule

Calculate the vector $Z1_i^{iter}$ & $Z2_i^{iter}$ using equation 23

Step 3.   Vector Combining

Calculate the vector U_i^{iter} using equation 25

Step 4.   Local Search

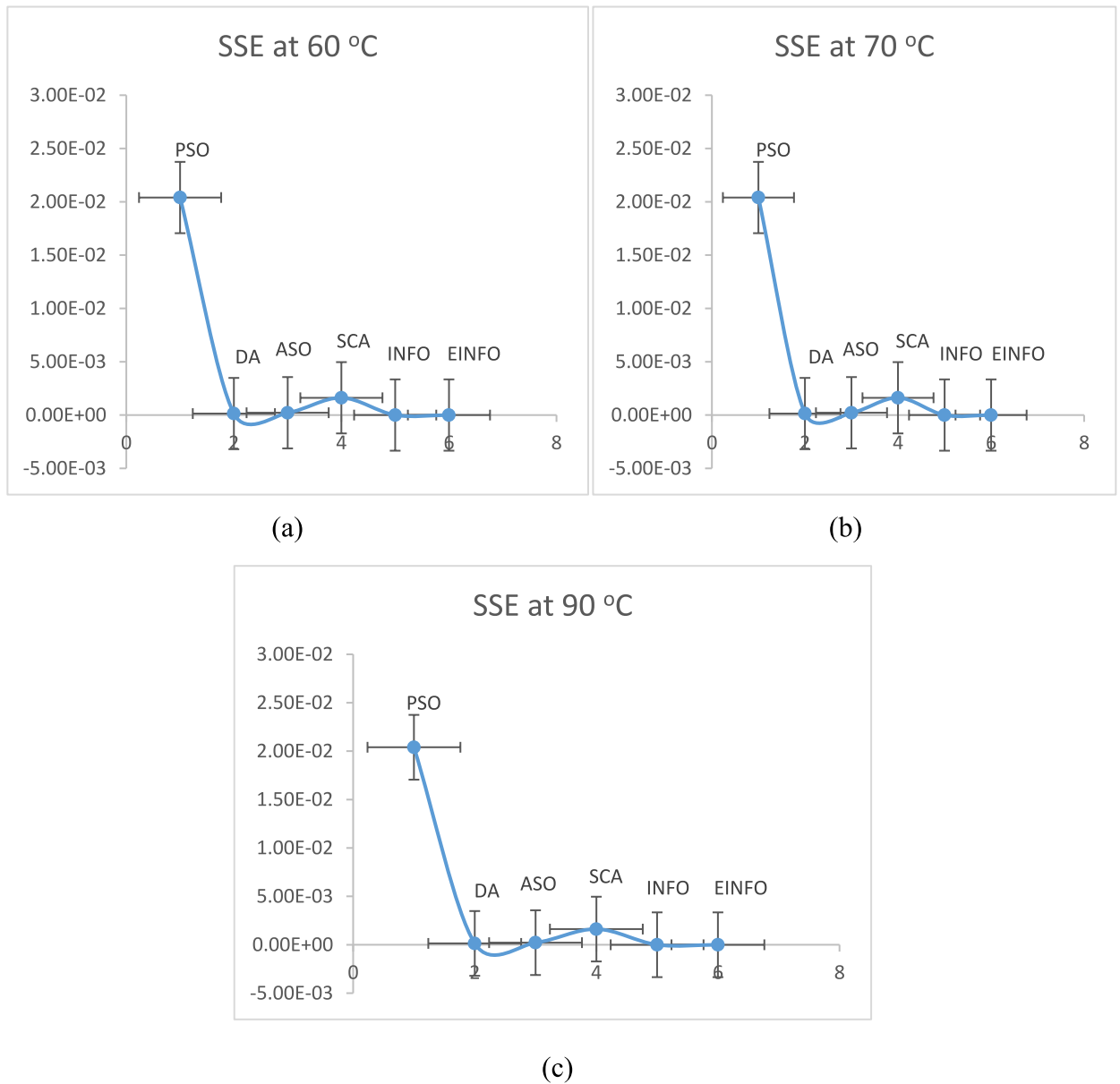Calculate the local search operate using equation 26

Fig. 6. (a) Sum of Square Error at 60 °C (b) 70 °C (c) 90 °C.

Step 5. High & low velocity ratio

    for iter <1/3 iter max
    Calculate the high velocity ration using equation 27
    Update the best vector
    then
    for iter >1/3 iter max
    Calculate the low velocity ration using equation 29
    Update the best vector

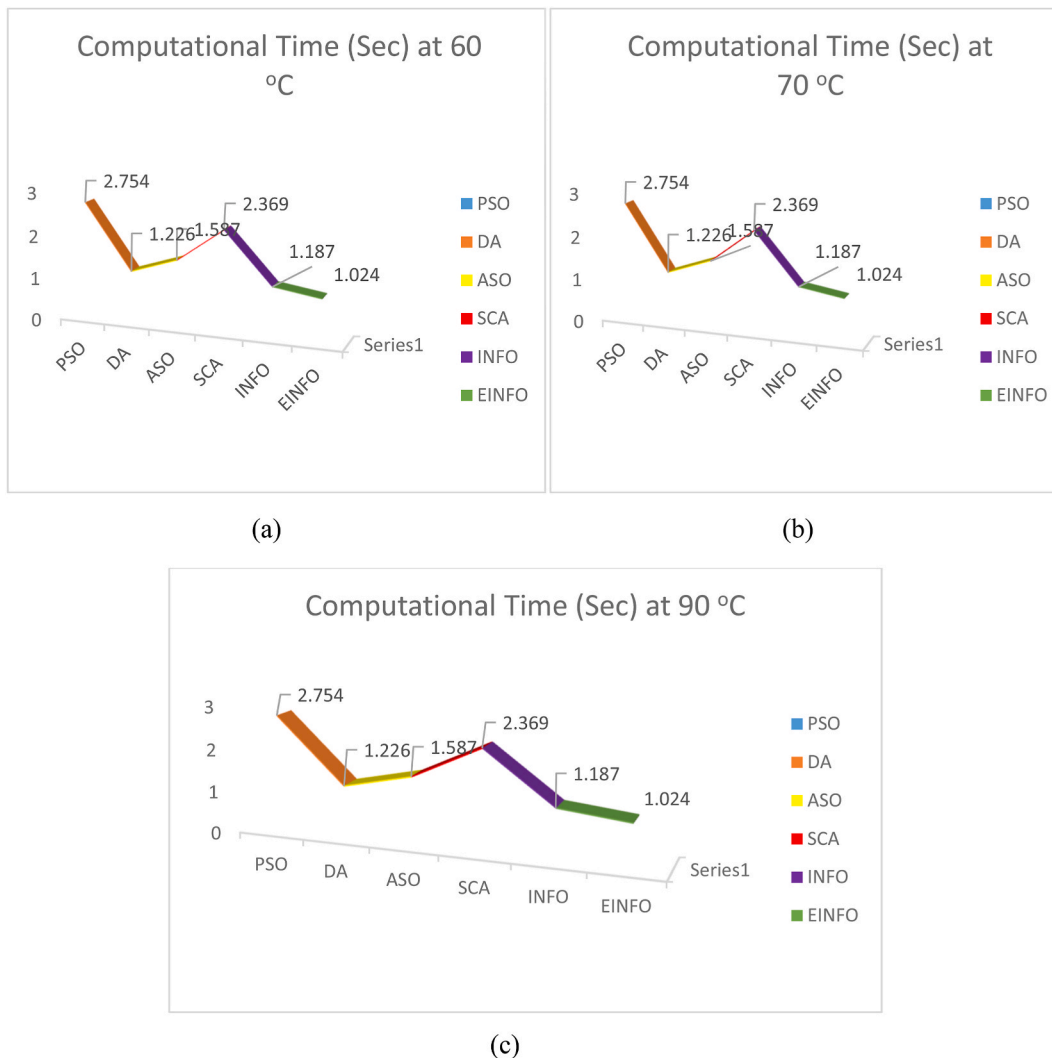**Step 6.** Return Vector $X_{best.j}^{g}$ as the final solution

(a)

(b)

(c)

Fig. 7. (a) Computational Time at 60 °C (b) 70 °C (c) 90 °C.

4. Results and discussion

The recently utilized metaheuristic algorithms PSO [32], DA [33], ASO [34], SCA [35], and INFO [28] are used to validate the proposed algorithm. The technical and operational data of the tested stack are displayed in Table 1. Table 2 displays the boundaries of the control variables for the DMFC stack. The estimated values of the control variables (e_o, α, r, j_{eid}, C_1, β,r_{eq}) were calculated by resolving the optimization problem. In order to produce a precise DMFC stack model, these properties will be used.
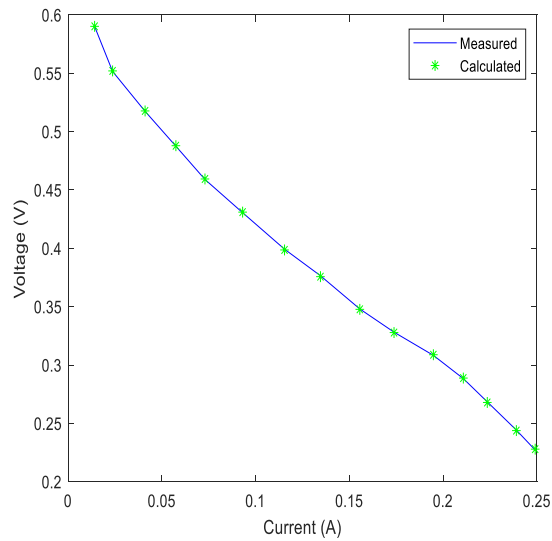
4.1. DMFC parameter estimation

Every programme has been coded in MATLAB 2020a and has been executed 20 times. All the algorithms are iterated at the same of search agents i.e. 30 and maximum no of iterations i.e. 1000 whereas the rest of the parameters of all the algorithms are kept standard. The suggested EINFO is used to estimate the parameters of DMFCs, and its performance and efficiency are further evaluated in comparison to a number of other algorithms, including PSO, INFO, DA, SCA, and ASO. The DMFC parameter estimation at STC (Standard Temperature Condition), with SSE and computation time is shown in Table 3. Fig. 4 shows, the sum of square error, standard deviation, I–V and P–V graph and computation time at standard temperature condition. The suggested approach outperforms the other comparable metaheuristic algorithms, it may be shown from these scattering figures. Table 4 displays the DMFC's statistics results. The DMFC convergence curve at STC is shown in Fig. 5. The suggested method outperforms the other examined algorithms, according to this figure.
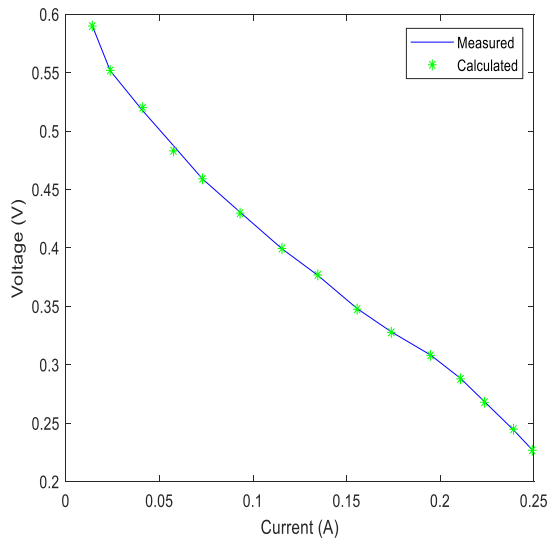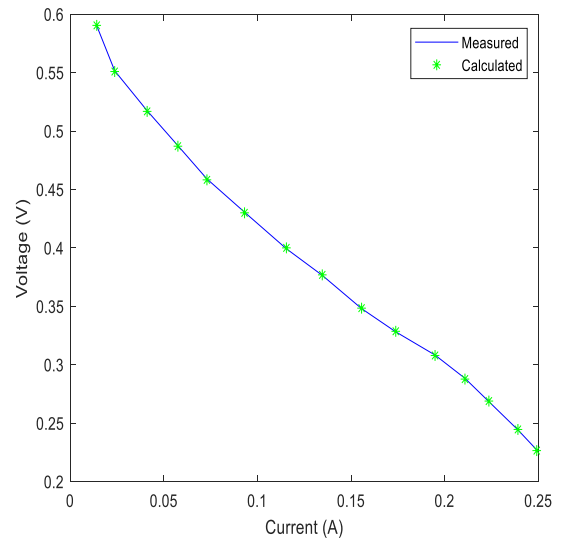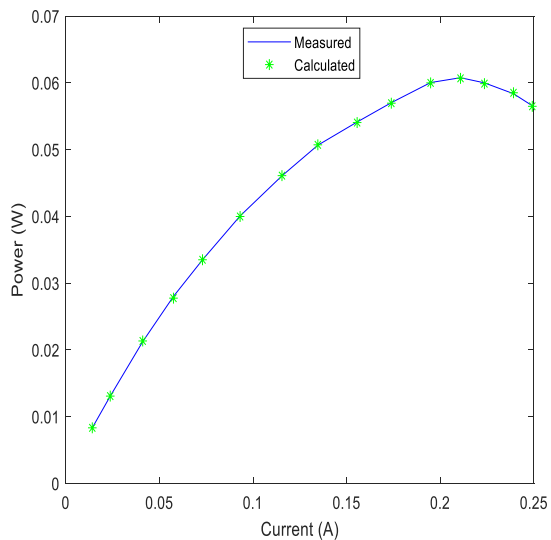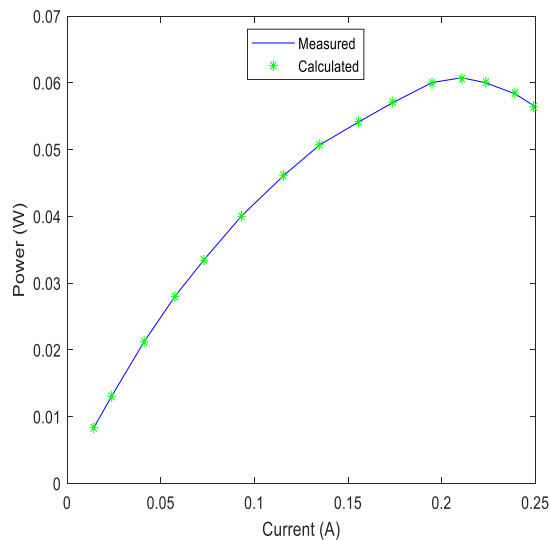
Fig. 8. (a) I–V Graph at 60 °C (b) 70 °C (c) 90 °C.

4.2. Convergence analysis

The parameter estimation for the DMFC at various operating temperatures is shown in Table 5. The parameter is extracted at different temperature i.e. 60, 70 and 90 °C respectively. At different temperature SSE and computation time is calculated as represented in Table 5. According to this table, the suggested method performs much better than the rest of the examined algorithms in terms of SSE and calculation time. Fig. 5 shows the convergence curve at various temperatures. This shows that the suggested hybrid method is more accurate and precise than existing meta-heuristic algorithms because of its faster rate of convergence. The SSE at various temperatures is seen in Fig. 6. Additionally, it may be inferred from this that the suggested method is superior to the rest of the algorithms evaluated. Fig. 7 shows the computational time at various operating temperatures, and it can be inferred that the suggested method performs significantly better than existing algorithms from this as well. Figs. 8 and 9 represents the I–V graphs and I–P graphs at different operating temperature of the proposed algorithm respectively.
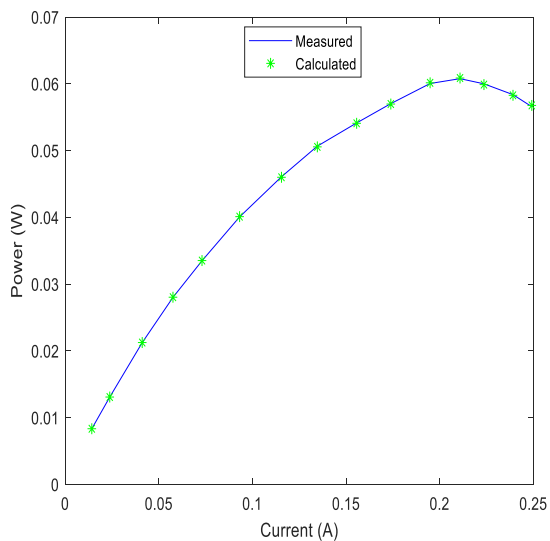
Fig. 9. (a) I–P Graph at 60 °C (b) 70 °C (c) 90 °C.

Table 6
Friedman ranking test.

Algorithm	Friedman ranking
Proposed Algorithm	1
INFO	2
SCA	5
ASO	4
DA	3
PSO	6

Table 7

Wilcoxon rank sum test.

Algorithm	INFO	DA	ASO	SCA	PSO
Proposed Algorithm	2.0104e-12	2.0123e-12	2.0142e-12	2.0180e-12	1.9822e-12

4.3. Non-parametric test

Based on the Friedman Ranking Test [36–39], Table 6 compares the parameter estimation of DMFC using the proposed algorithm with INFO, DA, ASO, SCA, and PSO respectively. It is evident from the results that the proposed algorithm is more efficient, accurate, precise, and robust than various other meta-heuristic algorithms. Second, the Wilcoxon rank sum test is applied in this test. It seems to be a simple, yet secure, and reliable non-parametric method for combined statistical analysis when samples are independent, and it is prominent and present in dynamic programming, as shown in Table 7.

5. Conclusion

The paper proposes a newly developed algorithm, EINFO, for obtaining the optimal solution to the DMFC parameter estimation optimization problem. Based on the results obtained, the following conclusions were drawn:

1. A new algorithm i.e., EINFO algorithm has been proposed.
2. At Standard Temperature Conditions, Parameter Estimation of DMFC is performed using EINFO, and the results show that the proposed hybrid algorithm offers better performance and more accuracy than various other meta-heuristic algorithms, including the SSE and computational time.
3. This study presents a convergence graph and different operating temperature curves which clearly demonstrate one of the highest speed of convergence of the proposed algorithm over other meta-heuristic algorithms.
4. In addition, a complete statistical analysis was conducted using Friedman Ranking Test and Wilcoxon rank sum test methods to demonstrate the efficiency, performance, and robustness of the proposed algorithm, with EINFO securing a first place ranking thus indicating that EINFO is the most effective.

The proposed algorithm has better performance than various other meta-heuristic algorithms, as it is more accurate and precise. The application of this method can be explored in other areas for better results. This proposed algorithms cam be solved to different complex engineering problems like parameter estimation of solar PV, optimal sizing of renewable energy system, thermal scheduling, etc.

Author contribution statement

Manish Kumar Singla: Performed the experiments; Analyzed and interpreted the data; Wrote the paper.
Jyoti Gupta: Analyzed and interpreted the data.
Parag Nijhawan: Conceived and designed the experiments.
Mohammed H. Alsharif: Performed the experiments.
Mun Kyeom Kim: Conceived and designed the experiments; Contributed reagents, materials, analysis tools or data.

Funding statement

Data availability statement

The data that has been used is confidential.

Declaration of interest's statement

The authors declare no conflict of interest.

References

[1] S.R. Yousefi, H.A. Alshamsi, O. Amiri, M. Salavati-Niasari, Synthesis, characterization and application of Co/Co$_3$O$_4$ nanocomposites as an effective photocatalyst for discoloration of organic dye contaminants in wastewater and antibacterial properties, J. Mol. Liq. 337 (2021), 116405.
[2] S.R. Yousefi, A. Sobhani, H.A. Alshamsi, M. Salavati-Niasari, Green sonochemical synthesis of BaDy$_2$ NiO$_5$/Dy$_2$ O$_3$ and BaDy$_2$ NiO$_5$/NiO nanocomposites in the presence of core almond as a capping agent and their application as photocatalysts for the removal of organic dyes in water, RSC Adv. 11 (19) (2021) 11500–11512.

[3] S.R. Yousefi, D. Ghanbari, M. Salavati-Niasari, M. Hassanpour, Photo-degradation of organic dyes: simple chemical synthesis of Ni (OH)$_2$ nanoparticles, Ni/Ni (OH)$_2$ and Ni/NiO magnetic nanocomposites, J. Mater. Sci. Mater. Electron. 27 (2) (2016) 1244–1253.

[4] A.A. Kulikovsky, The voltage–current curve of a direct methanol fuel cell:"exact" and fitting equations, Electrochem. Commun. 4 (12) (2002) 939–946.

[5] H. Guo, C.F. Ma, 2D analytical model of a direct methanol fuel cell, Electrochem. Commun. 6 (3) (2004) 306–312.

[6] J.P. Meyers, B. Bennett, Analytical model to relate DMFC material properties to optimum fuel efficiency and system size, J. Power Sources 196 (22) (2011) 9473–9480.

[7] N.S. Rosenthal, S.A. Vilekar, R. Datta, A comprehensive yet comprehensible analytical model for the direct methanol fuel cell, J. Power Sources 206 (2012) 129–143.

[8] H. Deng, J. Chen, K. Jiao, X. Huang, An analytical model for alkaline membrane direct methanol fuel cell, Int. J. Heat Mass Tran. 74 (2014) 376–390.

[9] P. Argyropoulos, K.E.I.T.H. Scott, A.K. Shukla, C. Jackson, A semi-empirical model of the direct methanol fuel cell performance: Part I. Model development and verification, J. Power Sources 123 (2) (2003) 190–199.

[10] R. Ben Messaoud, S. Hajji, Parameter extraction and mathematical modelling of the DMFC using Salp Swarm Algorithm, Polym. Bull. (2022) 1–18.

[11] Y. Wang, J.P. Zheng, G. Au, E.J. Plichta, A semi-empirical method for electrically modeling of fuel cell: executed on a direct methanol fuel cell, ECS Trans. 12 (1) (2008) 221.

[12] Q. Yang, A. Kianimanesh, T. Freiheit, S.S. Park, D. Xue, A semi-empirical model considering the influence of operating parameters on performance for a direct methanol fuel cell, J. Power Sources 196 (24) (2011) 10640–10651.

[13] T. Selyari, A.A. Ghoreyshi, M. Shakeri, G.D. Najafpour, T. Jafary, Measurement of polarization curve and development of a unique semiempirical model for description of PEMFC and DMFC performances, Chem. Indu. Chem. Eng. Quart. CICEQ 17 (2) (2011) 207–214.

[14] J. Ge, H. Liu, A three-dimensional mathematical model for liquid-fed direct methanol fuel cells, J. Power Sources 160 (1) (2006) 413–421.

[15] U. Krewer, M. Pfafferodt, A. Kamat, D.F. Menendez, K. Sundmacher, Hydrodynamic characterisation and modelling of anode flow fields of Direct Methanol Fuel Cells, Chem. Eng. J. 126 (2–3) (2007) 87–102.

[16] W.W. Yang, T.S. Zhao, A transient two-phase mass transport model for liquid feed direct methanol fuel cells, J. Power Sources 185 (2) (2008) 1131–1140.

[17] Z. Miao, Y.L. He, X.L. Li, J.Q. Zou, A two-dimensional two-phase mass transport model for direct methanol fuel cells adopting a modified agglomerate approach, J. Power Sources 185 (2) (2008) 1233–1246.

[18] J. Ko, P. Chippar, H. Ju, A one-dimensional, two-phase model for direct methanol fuel cells–Part I: model development and parametric study, Energy 35 (5) (2010) 2149–2159.

[19] P. Chippar, J. Ko, H. Ju, A global transient, one-dimensional, two-phase model for direct methanol fuel cells (DMFCs)–Part II: analysis of the time-dependent thermal behavior of DMFCs, Energy 35 (5) (2010) 2301–2308.

[20] S.J. Wang, W.W. Huo, Z.Q. Zou, Y.J. Qiao, H. Yang, Computational simulation and experimental evaluation on anodic flow field structures of micro direct methanol fuel cells, Appl. Therm. Eng. 31 (14–15) (2011) 2877–2884.

[21] D. Ouellette, A. Ozden, M. Ercelik, C.O. Colpan, H. Ganjehsarabi, X. Li, F. Hamdullahpur, Assessment of different bio-inspired flow fields for direct methanol fuel cells through 3D modeling and experimental studies, Int. J. Hydrogen Energy 43 (2) (2018) 1152–1170.

[22] D.P. Mahato, J.K. Sandhu, N.P. Singh, V. Kaushal, On scheduling transaction in grid computing using cuckoo search-ant colony optimization considering load, Cluster Comput. 23 (2020) 1483–1504.

[23] S. Rani, H. Babbar, P. Kaur, M.D. Alshehri, S.H.A. Shah, An optimized approach of dynamic target nodes in wireless sensor network using bio inspired algorithms for maritime rescue, in: IEEE Trans. Intell. Transport. Syst., 2022.

[24] K. Priya, T.S. Babu, K. Balasubramanian, K.S. Kumar, N. Rajasekar, A novel approach for fuel cell parameter estimation using simple genetic algorithm, Sustain. Energy Technol. Assessments 12 (2015) 46–52.

[25] K. Priya, K. Sathishkumar, N. Rajasekar, A comprehensive review on parameter estimation techniques for Proton Exchange Membrane fuel cell modelling, Renew. Sustain. Energy Rev. 93 (2018) 121–144.

[26] Y. Xing, J. Na, R. Costa-Castelló, Adaptive online parameter estimation algorithm of PEM fuel cells, in: 2019 18th European Control Conference (ECC), IEEE, 2019, June, pp. 441–446.

[27] J. Kim, S.M. Lee, S. Srinivasan, C.E. Chamberlin, Modeling of proton exchange membrane fuel cell performance with an empirical equation, J. Electrochem. Soc. 142 (8) (1995) 2670.

[28] R. Govindarasu, S. Somasundaram, Studies on influence of cell temperature in direct methanol fuel cell operation, Processes 8 (3) (2020) 353.

[29] I. Ahmadianfar, A.A. Heidari, S. Noshadian, H. Chen, A.H. Gandomi, INFO: an efficient optimization algorithm based on weighted mean of vectors, Expert Syst. Appl. 195 (2022), 116516.

[30] A. Faramarzi, M. Heidarinejad, S. Mirjalili, A.H. Gandomi, Marine predators algorithm: a nature-inspired metaheuristic, Expert Syst. Appl. 152 (2020), 113377.

[31] M.H. Hassan, D. Yousri, S. Kamel, C. Rahmann, A modified Marine predators algorithm for solving single-and multi-objective combined economic emission dispatch problems, Comput. Ind. Eng. 164 (2022), 107906.

[32] F. Marini, B. Walczak, Particle swarm optimization (PSO). A tutorial, Chemometr. Intell. Lab. Syst. 149 (2015) 153–165.

[33] S. Mirjalili, Dragonfly algorithm: a new meta-heuristic optimization technique for solving single-objective, discrete, and multi-objective problems, Neural Comput. Appl. 27 (4) (2016) 1053–1073.

[34] L.L. Li, Y.B. Chang, M.L. Tseng, J.Q. Liu, M.K. Lim, Wind power prediction using a novel model on wavelet decomposition-support vector machines-improved atomic search algorithm, J. Clean. Prod. 270 (2020), 121817.

[35] S. Mirjalili, SCA: a sine cosine algorithm for solving optimization problems, Knowl. Base Syst. 96 (2016) 120–133.

[36] J. Gupta, P. Nijhawan, S. Ganguli, Optimal parameter estimation of PEM fuel cell using slime mould algorithm, Int. J. Energy Res. 45 (10) (2021) 14732–14744.

[37] J. Gupta, P. Nijhawan, S. Ganguli, Parameter estimation of fuel cell using chaotic mayflies optimization algorithm, Adv. Theor. Simul. 4 (12) (2021), 2100183.

[38] B. Singh, P. Nijhawan, M.K. Singla, J. Gupta, P. Singh, Hybrid algorithm for parameter estimation of fuel cell, Int. J. Energy Res. 46 (8) (2022) 10644–10655.

[39] M.K. Singla, J. Gupta, P. Nijhawan, Solid oxide fuel cell parameter estimation using enhanced LSHADE algorithm and Newton Raphson method, Int. J. Energy Res. 46 (15) (2022) 23341–23352.